Acta Crystallographica Section D
Biological Crystallography
ISSN 0907-4449

Crystallization and preliminary X-ray crystallographic studies on the *parD*-encoded protein Kid from *Escherichia coli* plasmid R1

David Hargreaves,[a] Rafael Giraldo,[b] Sandra Santos-Sierra,[b] Rolf Boelens,[c] David W. Rice,[a] Ramón Díaz Orejas[b] and John B. Rafferty[a]*

[a]Krebs Institute for Biomolecular Research, Department of Molecular Biology and Biotechnology, The University of Sheffield, Sheffield S10 2TN, England, [b]Centro de Investigaciones Biológicas, Department of Molecular Microbiology, Velázquez 144, E-28006 Madrid, Spain, and [c]Bijvoet Centre for Biomolecular Research, Utrecht University, Padualaan 8, 3584 CH Utrecht, The Netherlands

Correspondence e-mail: j.rafferty@sheffield.ac.uk

Received 11 September 2001
Accepted 3 December 2001

DNA replication in *Escherichia coli* and therefore bacterial proliferation relies upon the efficient functioning of the DnaB helicase. The toxin protein Kid from the plasmid-stability system *parD* encoded on plasmid R1 of *E. coli* is thought to target and block DnaB-dependent DNA replication. The toxicity of Kid is antagonized through interaction with the Kis antidote protein and the resultant complex can then act as a transcriptional regulator for the *parD* system. Crystals of selenomethionine-incorporated Kid have been obtained by the hanging-drop vapour-diffusion method using potassium phosphate as the precipitant. The crystals belong to the monoclinic system, space group $P2_1$, have unit-cell parameters $a = 32.9$, $b = 45.0$, $c = 64.4$ Å, $\beta = 96.2^\circ$ and diffract to a $d_{\rm min}$ of better than 1.8 Å on a synchrotron-radiation source. The determination of the structure of Kid will permit a better understanding of its interactions with DnaB and Kis and allow the evolutionary relationships of Kid to other toxins of plasmid and chromosomal origin to be explored.

1. Introduction

In prokaryotes, stable plasmid inheritance mainly arises from specific gene cassettes whose protein products fall into three main classes: (i) centromere-like structures which distribute replicon copies within the cell prior to division, (ii) site-specific recombinases that resolve multimeric plasmids and (iii) post segregational killing (PSK) systems that kill plasmid-free progeny (Gerdes, 2000 and references therein). In general, the PSK mechanism functions *via* two small plasmid-encoded proteins, a stable toxin and a short-lived antagonist that binds to the toxin and inactivates it. The instability of the antagonist requires the organism to replenish its cellular supply constantly, which is not possible if progeny have not inherited the plasmid. In this scenario, the antagonist is degraded, often by a specific protease, leaving the toxin free to act at its target, resulting in cell death.

Plasmid R1 carries the PSK locus *parD*, which comprises an operon with two genes, *kis* and *kid* (Bravo *et al.*, 1987), coding for the small toxin protein Kid (killing determinant) and the antagonist Kis (killing suppresser) that neutralizes the toxicity of Kid (Bravo *et al.*, 1988). In the case of the *parD* system, the protease responsible for the degradation of the antagonist (Kis) is Lon (Tsuchimoto *et al.*, 1992). Together Kis and Kid act as a transcriptional repressor at the promoter of *parD* (Ruiz-Echevarría, Berzal-Gerranz *et al.*, 1991). Kid and Kis are also found perfectly conserved in the *pem* (plasmid emergency maintenance) PSK system of plasmid R100 (Tsuchimoto *et al.*, 1988; Tsuchimoto & Ohtsubo, 1993). Homologous systems to *parD*/*pem* have been found in the chromosome of *E. coli* (Masuda *et al.*, 1993) and in many other Gram-negative and Gram-positive bacteria (Gerdes, 2000).

Purified Kid protein has been shown to specifically inhibit initiation of DnaB-dependent DNA replication in cell-free extracts of *E. coli* (Ruiz-Echevarría *et al.*, 1995). This clearly differentiates the toxin of the *parD* system from that of the *E.coli ccd* PSK system, where the killer component, CcdB, whose crystallographic structure is known (Loris *et al.*, 1999), poisons the DNA topoisomerase II (Bernard & Couturier, 1992; Maki *et al.*, 1992). There is significant sequence similarity between the antagonists (Kis/CcdA) of both systems, but none between the agonists (Kid/CcdB), which further suggests that they have different targets (Ruiz-Echevarría, de Torrontegui *et al.*, 1991). Toxin–antitoxin plasmid maintenance systems are widespread amongst bacteria and this has lead to interest in their molecular mechanisms. Currently the $\omega\varepsilon\zeta$ plasmid-maintenance system of *Streptococcus pyrogenes* is also the subject of preliminary crystallographic studies (Meinhart *et al.*, 2001).

In order to understand the molecular basis of the interactions of Kid with DnaB and Kis, a detailed crystallographic analysis of Kid has

© 2002 International Union of Crystallography
Printed in Denmark – all rights reserved

been undertaken with a view, in the longer term, to the development of novel anti-infective agents.

2. Materials and methods

Selenomethionine-incorporated Kid protein (SeMet-Kid) was prepared with a view to performing MAD phasing experiments using the three available selenomethionine-incorporation sites present in each monomer (GenBank Accession number X06240). Cloning was achieved in *E. coli* strain C600 using the vector pRG-recA-NHis (Giraldo *et al.*, 1998), which carries the genes for Kid and a hexahistidine-tagged Kis. The co-expression of Kis and Kid was necessary to attenuate the cytotoxic action of Kid. Furthermore, the inclusion of the hexahistidine-tagged Kis allowed efficient separation of the heterodimer from the crude cell lysate. Initial selection of the 6His-Kis/Kid clone was achieved by plating a frozen glycerol stock onto LB agar containing 100 µg ml^{-1} ampicillin and growing overnight at 310 K (Sambrook *et al.*, 1989). A single colony was selected and used to inoculate 50 ml of LB containing 100 µg ml^{-1} ampicillin, which was then grown overnight at 310 K in a shaking incubator. The overnight culture was then used to inoculate two 2 l flasks each containing 500 ml of sterile LB (100 µg ml^{-1} ampicillin) and shaken at 310 K until the turbidity reached OD_{600} = 1.0. The contents of the two flasks were then transferred into a sterile centrifuge bottle and centrifuged at 4200 rev min^{-1} for 10 min at room temperature. The supernatant was then discarded and the cell pellet resuspended in 50 ml of fresh sterile LB containing 100 µg ml^{-1} ampicillin. The 50 ml of concentrated cell suspension was then used to inoculate a small bench-top fermenter containing 3.5 l of supplemented minimal media containing 100 µg ml^{-1} ampicillin at 310 K. The turbidity of the culture was then monitored closely to ensure growth remained in the logarithmic phase until an OD_{600} of 0.8 was reached (starting OD_{600} = 0.35). At this point, selenomethionine (21 µg ml^{-1}) and nalidixic acid (25 µg ml^{-1}) were added to the culture along with extra ampicillin equating to half the amount used at the start of fermentation. The culture was then fermented overnight at 310 K before harvesting the cells by centrifugation at 4200 rev min^{-1} and 277 K. The cell paste was then washed in 6–8 ml of storage buffer [50 m*M* Tris–HCl pH 8.0, 100 m*M* NaCl, 1 m*M* EDTA, 5%(*v*/*v*) glycerol] and centrifuged at 277 K to form a firm pellet. The supernatant was then discarded and the cell paste frozen at 253 K for future use. Analysis of pre- and post-induction samples using SDS–PAGE showed strong post-expression bands at approximately 10 and 12 kDa, corresponding to the 6His-Kis and Kid proteins, respectively.

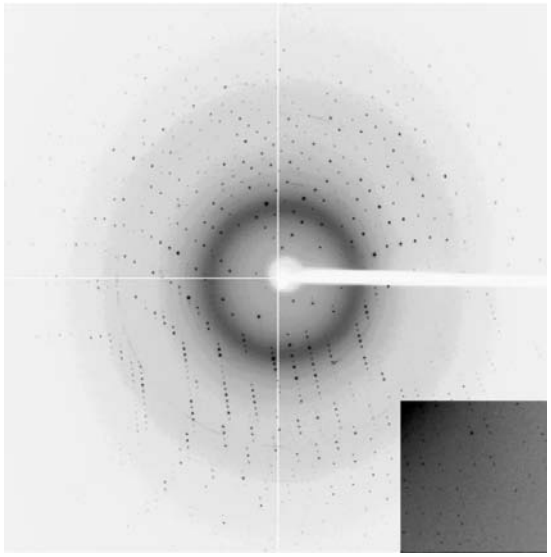

Figure 1
A representative 2° rotation image taken from a frozen crystal of *E. coli* selenomethionine-incorporated Kid on beamline 14.4 at the European Synchrotron Radiation Facility. Diffraction at the edge of the plate has a d_{min} of approximately 1.5 Å which extends to approximately 1.25 Å at the corners (inlay, enhancement of the plate corner).

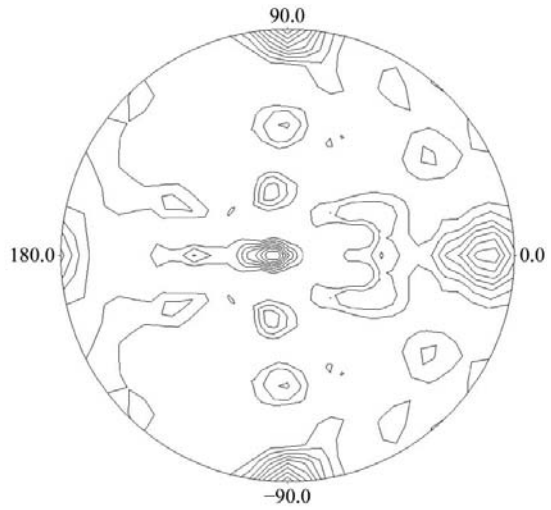

Figure 2
A stereographic representation of the $\kappa = 180°$ section of the self-rotation function of the *E. coli* selenomethionine Kid calculated using data between 20 and 3 Å with a radius of integration 10 Å. The two peaks at $\omega = 83, \varphi = 0.0°$ and $\omega = 7, \varphi = 180.0°$ represent two possible positions of the non-crystallographic twofold axis of the Kid dimer. The appearance of two peaks is consistent with the presence of a dimer in the asymmetric unit in which the non-crystallographic twofold axis lies in the *ac* plane.

In order to purify the SeMet-Kid, the cell pellet from the 3.5 l of culture was defrosted at room temperature and washed in 0.9%(*w*/*v*) NaCl. The cells were then suspended in lysis buffer [1 *M* KCl, 20 m*M* imidazole pH 8.0, 1% Brij, 1 m*M* *p*-aminobenzamidine, 10%(*v*/*v*) glycerol] and sonicated on ice for four cycles of 45 s in an MSE sonicator at 60% amplitude. The lysate was then clarified by centrifugation for 60 min at 15 000 rev min^{-1} and 277 K. The soluble fraction was then loaded at 1 ml min^{-1} onto an Ni-affinity column [10 ml of Chelating Sepharose Fast-Flow packed into a XK-16/20 column (Pharmacia) and activated with excess $NiCl_2$] that had been equilibrated previously with ten column volumes of buffer *A* (1 *M* KCl, 20 m*M* imidazole pH 8.0). The column was then washed with buffer *A* until the OD_{280} reached a constant baseline reading. Denatured Kid was then eluted from the Ni-6His-Kis/Kid complex using 5 *M* guanidine–HCl, 20 m*M* imidazole–HCl at pH 8.0. The total yield of Kid from the overexpression and initial purification was estimated to be 60 mg and subsequent electrospray mass-spectrometric analysis of the SeMet-Kid protein suggested that the average incorporation of selenium was 80%.

Refolding was accomplished using the dialysis method. Approximately 10–20 mg of Kid was diluted to 100 ml using a buffer consisting of 5.6 *M* guanidine–HCl, 0.56 *M* $(NH_4)_2SO_4$, 200 m*M* ammonium acetate, 20 m*M* β-mercaptoethanol, 0.2 m*M* EDTA and 1.2%(*w*/*v*) CHAPS (pH adjusted to 6.0 using NH_4OH). The 100 ml of protein solution was then dialysed using a 10 kDa cutoff dialysis membrane at 277 K against four changes of buffer (5 l in total) consisting of 0.5 *M* $(NH_4)_2SO_4$, 50 m*M* ammonium acetate, 10 m*M* β-mercaptoethanol, 0.1 m*M* EDTA and 5%(*v*/*v*) ethylene glycol adjusted to pH 6.0 with NH_4OH. The refolded Kid protein was then dialyzed against 5 l of 20 m*M* HEPES, 50 m*M* KCl pH 7.0 (four changes as above) and clarified by centrifugation at 15 000 rev min^{-1} for 30 min at

277 K. The supernatant was loaded at 1 ml min^{-1} flow rate onto an SP-Sepharose column (Pharmacia) equilibrated with 20 m*M* HEPES, 50 m*M* KCl pH 7.0. After extensive washing, the bound Kid protein was eluted using a 250 ml linear KCl gradient (50–500 m*M*). Peak fractions from the SP-Sepharose column were analysed by SDS–PAGE and those containing the purest Kid samples were pooled and concentrated by filtration at 277 K in an Amicon 50 ml cell fitted with a Diaflo PM-10 membrane. Finally, the sample was stored at 255 K after adding β-mercaptoethanol and ethylene glycol to final concentrations of 20 m*M* and 5%(*v*/*v*), respectively.

In order to verify that the refolding of Kid had been successful, an *in vitro* assay was performed which showed that the refolded protein inhibited DnaB-dependent ColE1 replication (data not shown). Refolded Kid was also seen to form an active complex with the refolded Kis antidote that interacted with specific oligonucleotide sequences on the *parD* promoter in the same way as the native Kis/Kid complex. Furthermore, comparison of the native and refolded Kis/Kid complexes using analytical centrifugation showed that both species had a molecular weight of 84 kDa, approximating to an octameric quaternary arrangement, under the same conditions (data not shown).

For crystallization, selenomethionine-incorporated Kid previously stored at 255 K was extensively dialysed against 100 m*M* potassium phosphate pH 5.8 at 277 K. The dialysed protein was then concentrated using a 10 kDa centrifugal concentrator until the protein concentration was approximately 2–2.5 mg ml^{-1} as measured using a Bradford assay (Bradford, 1976). The protein solution was then treated with a proprietary protease-inhibitor cocktail (Roche, Complete Protease Inhibitor) according to the instructions supplied with the product. Crystallization was accomplished using the hanging-drop vapour-diffusion method. Small drops of protein solution were suspended over wells containing concentrations of NaCl varying from 0.4 to 1.5 *M*. Crystals with a plate-like morphology and overall dimensions of approximately 0.2 × 0.2 × 0.05 mm grew within 24 h and reached maximum dimensions of 0.6 × 0.6 × 0.1 mm after a few days.

Crystals of SeMet-Kid were successfully cryoprotected using Paratone-N for data collection at 100 K. Multiple-wavelength anomalous dispersive data were collected to a $d_{\min}$ of 1.8 Å from a single crystal on beamline 14.4 at the ESRF. Three data sets, E_1, E_2 and E_3, were collected using 2° rotations and 2 s exposures on an ADSC CCD detector at wavelengths λ = 0.97965 ($f''_{\rm maximum}$), λ = 0.97979 ($f'_{\rm minimum}$) and λ = 0.968633 Å (high-energy remote), respectively, relative to the selenium *K* edge as determined from a fluorescence absorption spectrum obtained from the crystal. The crystal survived these exposures without noticeable radiation damage, so a fourth data set (E_4) was collected to a $d_{\min}$ of 1.4 Å at a low-energy wavelength (λ = 0.98400 Å) using 1° rotations and 2 s exposures.

Table 1
Data-collection statistics for the selenomethionine Kid data collected from a single crystal at four wavelengths at station ID 14.4 at the ESRF, Grenoble, France.

Values in parentheses refer to the outer resolution shell.

	E_1	E_2	E_3	E_4
Resolution (Å)	20–1.8 (1.84–1.80)	20–1.8 (1.84–1.80)	20–1.8 (1.84–1.80)	20–1.4 (1.43–1.4)
$R_{\rm merge}$ (%)	6.60 (11.20)	3.70 (7.10)	5.20 (11.30)	4.20 (10.70)
$I/\sigma(I) > 3$ (%)	96.50 (90.90)	96.40 (95.60)	95.20 (87.50)	95.30 (87.40)
Completeness (%)	95.40 (71.10)	86.20 (43.20)	95.50 (72.20)	96.10 (73.70)
Wavelength (Å)	0. 97965	0.97979	0.968633	0.98400
Redundancy	3.4 (2.2)	1.9 (1.8)	3.4 (2.2)	3.2 (1.6)
Overall mosaicity (°)	0.55	0.55	0.57	0.58

3. Results and discussion

The data collected at the ESRF were processed and scaled using the *DENZO*/*SCALEPACK* package (Otwinowski & Minor, 1997). Analysis of the low-energy diffraction data (E_4) using the autoindexing routine in the program *DENZO* showed that the crystals belong to the primitive monoclinic system, with unit-cell parameters a = 32.9, b = 45.0, c = 64.4 Å, $\alpha = \gamma = 90$, β = 96.2°. Reflections were observed along the 0k0 axis (b*) only where they satisfied the condition $k = 2n$, indicating that the crystals belonged to space group $P2_1$. Significant reflections were observed out to the edge of the detector (Fig. 1), with over 87.4% of the reflections in the last resolution bin (1.43–1.39 Å) having $I/\sigma(I) > 3$ and 93.0% of reflections in all resolution bins having $I/\sigma(I) > 3$. Considerations of the possible values of $V_{\rm M}$ suggested that the crystals contain either a monomer ($V_{\rm M}$ = 4.1 Å^3 Da^{-1}) or a dimer ($V_{\rm M}$ = 2.1 Å^3 Da^{-1}) in the asymmetric unit (Matthews, 1968).

A total of 135 529 measurements were made of 37 429 independent reflections for data in the resolution range 20–1.4 Å. Data processing gave an overall merging R factor of 4.2% (11.0% in the outer resolution shell) and showed the data to be 95.5% complete (71.2% in the outer resolution shell). Data sets E_1, E_2 and E_3 were processed in the same way and the statistics for all the data sets collected can be found in Table 1.

E_4 data between 20 and 3 Å were used in the calculation of a self-rotation function using the program *POLARRFN* (Kabsch, unpublished work; Collaborative Computational Project, Number 4, 1994) with a radius of integration of 10 Å. Analysis of the function showed strong peaks on the κ = 180° section at ω = 83, φ = 0.0° and ω = 7, φ = 180.0° (Fig. 2), which suggest the presence of non-crystallographic twofold rotation axes close to a* and c*. The appearance of two peaks is consistent with the presence of a dimer in the asymmetric unit in which the non-crystallographic twofold axis lies in the *ac* plane.

Our efforts are now being directed toward the elucidation of the Se-atom substructure that will lead to a full structure determination of the Kid protein.

We would like to thank the support staff at the European Synchrotron Radiation Facility for their assistance with the MAD data collection. This work was supported by grants from the EU (BIO4-CT98-0106 and QLK2-CT-2000-00634). RDO also acknowledges support from the Spanish Government (Grant BIO99-0859-C03-01). The Krebs Institute is a designated BBSRC Biomolecular Sciences Centre and a member of the North of England Structural Biology Centre (NESBIC). JBR is the Royal Society Olga Kennard Fellow.

References

Bernard, P. & Couturier, M. (1992). *J. Mol. Biol.* **226**, 735–745.
Bradford, M. M. (1976). *Anal. Biochem.* **72**, 248–254.
Bravo, A., Ortega, S., de Torrontegui, G. & Díaz, R. (1988). *Mol. Gen. Genet.* **215**, 146–151.
Bravo, A., de Torrontegui, G. & Díaz, R. (1987). *Mol. Gen. Genet.* **210**, 101–110.
Collaborative Computational Project, Number 4 (1994). *Acta Cryst.* D**50**, 760–763.
Gerdes, K. (2000). *J. Bacteriol.* **182**, 561–572.
Giraldo, R., Andreu, J. M. & Díaz-Orejas, R. (1998). *EMBO J.* **17**, 4511–4526.
Loris, R., Dao-Thi, M. H., Bahassi, E. M., Van Melderen, L., Poortmans, F., Liddington, R.,

Couturier, M. & Wyns, L. (1999). *J. Mol. Biol.* **285**, 1667–1677.
Maki, S., Takiguchi, S., Miki, T. & Horiuchi, T. (1992). *J. Biol. Chem.* **267**, 12244–12251.
Masuda, Y., Miyakaswa, K., Nishimura, Y. & Ohtsubo, E. (1993). *J. Bacteriol.* **175**, 6850–6856.
Matthews, B. W. (1968). *J. Mol. Biol.* **33**, 491–497.
Meinhart, A., Alings, C., Strater, N., Camacho, A. G., Alonso, J. C. & Saenger, W. (2001). *Acta Cryst.* D**57**, 745–747.
Otwinowski, Z. & Minor, W. (1997). *Methods Enzymol.* **276**, 307–326.
Ruiz-Echevarría, M. J., Berzal-Herranz, A., Gerdes, K. & Díaz-Orejas, R. (1991). *Mol. Microbiol.* **5**, 2685–2693.
Ruiz-Echevarría, M. J., de Torrontegui, G., Giménez-Gallego, G. & Díaz-Orejas, R. (1991). *Mol. Gen. Genet.* **225**, 355–362.
Ruiz-Echevarría, M. J., de Torrontegui, G., Giménez-Gallego, G., Sabariegos-Jareno, R. & Díaz-Orejas, R. (1995). *J. Mol. Biol.* **247**, 568–577.
Sambrook, J., Fritsch, E. F. & Maniatis, T. (1989). *Molecular Cloning: a Laboratory Manual*, 2nd ed. Cold Spring Harbor, NY, USA: Cold Spring Harbor Laboratory Press.
Tsuchimoto, S., Nishimura, Y. & Ohtsubo, E. (1992). *J. Bacteriol.* **174**, 4205–4211.
Tsuchimoto, S. & Ohtsubo, E. (1993). *Mol. Gen. Genet.* **237**, 81–88.
Tsuchimoto, S., Ohtsubo, H. & Ohtsubo, E. (1988). *J. Bacteriol.* **170**, 1461–1466.